Synthesis and Properties of MoAlB Composites Reinforced with SiC Particles

Weiwei Zhang
Beijing Jiaotong University
Shibo Li (shbli1@bjtu.edu.cn)
Beijing Jiaotong University https://orcid.org/0000-0002-4371-4885
Shuang Wu
Beijing Jiaotong University
Boxiang Yao
Beijing Jiaotong University
Shukai Fan
China Porcelain Fuchi (Suzhou) High Tech Nano Materials Co. Ltd
Guoping Bei
China Porcelain Fuchi (Suzhou) High Tech Nano Materials Co. Ltd
Wenbo Yu
Beijing Jiaotong University
Yang Zhou
Beijing Jiaotong University
Ying Wu
South University of Science and Technology: Southern University of Science and Technology
Sun-an Ding
South University of Science and Technology: Southern University of Science and Technology

Research Article

Keywords: SiC/MoAlB, Composites, Mechanical properties, Oxidation, Microstructure.

Posted Date: September 23rd, 2021

DOI: https://doi.org/10.21203/rs.3.rs-889494/v1

Version of Record: A version of this preprint was published at Journal of Advanced Ceramics on January 12th, 2022. See the published version at https://doi.org/10.1007/s40145-021-0543-5.

Abstract

To develop MoAlB advanced ceramic with improved mechanical properties and oxidation resistance, the use of SiC particles to reinforce MoAlB composites has been adopted. 5–15 vol.% SiC/MoAlB have been prepared and characterized. A flexural strength of 380 MPa and a Vickers hardness of 12.7 GPa were achieved in the 5 vol. %SiC/MoAlB composite, increased by 24% and 51%, respectively, as compared with those for MoAlB. Oxidation at 1200°C and 1300°C for 10 h in air showed that the 5 vol. %SiC/MoAlB composite has good oxidation resistance than MoAlB due to the formation of a dense and continuous scale composed of Al_2O_3 and SiO_2, which prevents oxygen inward diffusion and the evaporation of oxides. We expect that the general strategy of second phase reinforcing for materials will help to widen the applications of MoAlB.

1. Introduction

MoAlB is an attractive ternary boride in MAB phase family (where M is a transition metal, A is aluminium or zinc, and B is boron [1]) due not only to its ease of fabrication and densification at relatively lower temperatures (1050–1200 °C) but also to its excellent high temperature oxidation resistance as compared with the vast majority of binary transition metal borides which generally require high temperatures of > 1700°C to achieve full density and have poor oxidation resistance at temperatures above 1000°C [2].

So far, only MoAlB in the MAB phase family has been demonstrated with good oxidation resistance at temperatures below 1300°C due to the formation of a dense and continuous α-Al_2O_3 layer [2–4]. Its oxidation resistance is even better than Ti_2AlC and Cr_2AlC MAX phases at 1100 °C [5–7]. For example, the oxidation rate constant K_c of MoAlB is about 7.1×10^{-23} m^3/s at 1100 °C [4], lower than $1.0\text{-}1.8\times10^{-21}$ m^3/s for Ti_2AlC [5]. The thickness of α-Al_2O_3 layer formed on MoAlB at 1100 °C for 100 h is about 3 μm, close to that on fine-grained Cr_2AlC ceramic [6]. However, increasing oxidation temperature leads to the rapid mass gains. To further improve its oxidation resistance, the replacement of some Al by Si in MoAlB to form Mo(Al,Si)B solid solutions has been designed because the elemental Si can be oxidized to SiO_2 which retards the inner diffusion of O upon oxidation. The $MoAl_{0.97}Si_{0.03}B$ solid solution exhibited better oxidation resistance than MoAlB. In the temperature range 1200–1400 °C, the mass gain and the scale thickness of $MoAl_{0.97}Si_{0.03}B$ are lower than those of MoAlB [7]. The above results confirm that Si effectively improves the oxidation resistance of MoAlB. However, the solubility of Si in MoAlB is limited, with the maximum solubility of ~ 0.91 at.% [8], causing the difficult study of the influence of Si content on the oxidation behavior of MoAlB.

Another facile route to enhance the oxidation resistance of MoAlB is incorporation of ceramic particles. Among ceramics particles, SiC is preferred to reinforce MoAlB due to the following two reasons. First, SiC has a high melting point, high hardness, and excellent oxidation resistance. Second, SiC has been demonstrated to be a good reinforcement in the MAX composites. It has been proved that the

incorporation of SiC in Ti_3SiC_2 matrix is one of the simplest yet effective approaches to prepare composites with greatly improved mechanical properties and high temperature oxidation resistance [9–14].

In the present study, the main purpose is to prepare SiC/MoAlB composites with a combination of enhanced oxidation resistance and improved mechanical properties. The effect of SiC content on the properties of composites was investigated, the oxidation tests at high temperatures of 1200 ºC and 1300 ºC in air were performed, and the phase composition and microstructure of the prepared composites were characterized.

2. Experimental Details

2.1 Material preparation

To prepare MoAlB samples, Mo (-300 mesh, 99.5 % purity, General Research Institute for Nonferrous Metals, GRINM, China), Al (-300 mesh, 99.5 % purity, Beijing Reagent Company, China), and B (-300 mesh, 99 % purity, GRINM, China) powders with a molar ration of Mo:Al:B = 1:1.3:1 were mixed for 10 h, and then pressureless-sintered at 1200 ºC for 1 h in Ar atmosphere. The sintered samples were pulverized and then sieved with a 200 meshed sieve to prepare MoAlB powders.

To prepare SiC/MoAlB composites, SiC (an average size of ~ 28 μm, > 99 % purity, GRINM, China) and MoAlB powders were mixed for 10 h, and then hot pressed at 1200 ºC under 25 MPa for 1 h in Ar atmosphere. The volume contents of SiC are 5, 10, and 15 vol. %.

2.2 Mechanical property measurement

The prepared SiC/MoAlB samples were cut into bars with different sizes by a wire electrical discharge machine. The bars were polished to 1200 grit size with SiC papers, cleaned with ethanol, and then dried in an oven at 50°C for 4 h. The different-sized bars were used for mechanical property and oxidation tests.

3 mm × 4 mm × 36 mm bars were used to measure the flexural strength by the three-point bending test in a WDW-100E compression machine. The span size and crosshead speed were 30 mm and 0.5 mm/min, respectively.

The Vickers hardness test was performed in a TH700 hardness tester under loads of 1–20 kg with a dwelling time of 15 s. Six measurements in different areas were performed for each sample to obtain an average value.

2.3 Oxidation test

3 mm × 4 mm × 10 mm bars were used to investigate the oxidation behavior in a TSK-5-14 high temperature tube furnace at 1200 °C and 1300 °C for 10 hrs in air. The weight gain was measured at the interval of 2 h. The weight change of the samples was measured using an analytical balance with an

accuracy of 0.0001 g and converted into a specific weight change per surface area. The oxidized samples were used to the following microstructure and phase characterization.

2.3 Characterization

The phase compositions of mixtures, hot-pressed samples before and after oxidation were analyzed by X-ray diffraction (XRD) analysis using a Rigaku Ultima IV diffractometer with Cu Kα radiation (Kα = 0.154 nm) operated at 40 kV and 40 mA. The morphologies of mixture powders, polished and fractured surfaces of hot-pressed samples, and oxide scale were characterized with a ZEISS EVO 18 scanning electron microscope (SEM, Carl Zeiss SMT, Germany) equipped with an energy-dispersive spectrometer system (EDS).

For TEM examination, focused ion beam (FIB) cross-section was prepared with a dual-beam FIB/SEM (FEI Scios, USA) by using a Ga + ion source operating at 30 kV. A thin slice representing a cross-sectional cut perpendicular to the SiC/MoAlB boundary was analyzed by a FEI Talos F200X (FEI, USA) transmission electron microscope (TEM) with an operating voltage of 200 kV.

3. Results

3.1 Preparation and characterization of SiC/MoAlB composites

MoAlB composites reinforced with 5, 10, 15 vol. % SiC were prepared by hot pressing at 1200 ºC under 25 MPa for 1 h in Ar atmosphere. Figure 1 presents the XRD results for the prepared composites. The composites are primarily composed of MoAlB and SiC. In addition, weak peaks belonging to Al_3Mo appear in the XRD patterns. No new phases were found in the XRD patterns, indicating that there are no reactions occurring between SiC and MoAlB at the sintering temperature of 1200 °C. The back-scattered SEM micrograph (Fig. 2a) depicts the distribution of SiC particles (black color) with irregular shapes in the 10 vol.% SiC/MoAlB composite. Al_3Mo (light grey color in Fig. 1a) and Al_2O_3 (small black particles in Fig. 1b) as impurity phases were found, which should be from the initial MoAlB powder. No Al_2O_3 peaks were detected in the XRD patterns (Fig. 1), possibly due to its amount below the detection limit of XRD. An enlarged SEM image taken from the dashed rectangle area in Fig. 2a, clearly shows the boundary areas between SiC and MoAlB particles (Fig. 2b). There are neither new formed phases nor reaction layers in the boundary area, confirming the thermal stability of SiC with MoAlB at 1200°C.

TEM observations were performed to further examine the microstructure of the 5 vol.% SiC/MoAlB composite. Figure 3 (a) shows the TEM analysis of one representative SiC/MoAlB phase boundary. No reaction zones were observed in the phase boundary. A high resolution TEM (HRTEM) image presents the lattice fringes of SiC and MoAlB (Fig. 3b). The measured interplanar spacing is about 0.1822 nm, corresponding to the (102) plane of SiC; and 0.704 nm, corresponding to the (020) plane of MoAlB. The HRTEM image reveals that the interface is clean and continuous, and neither new phases nor amorphous

phases are formed at the interface. The above observation suggests that SiC particles are chemically stable with the MoAlB matrix at the sintering temperature of 1200°C.

3.2 Mechanical properties

The measured mechanical properties as a function of reinforcing phase content are presented in Fig. 4. A flexural strength of 380 MPa and a Vickers hardness of 12.7 GPa have been successfully achieved in 5 vol. %SiC/MoAlB composite, increased by 24% and 51%, respectively, as compared with 306 MPa and 8.4 GPa for MoAlB material. However, both the strength and the hardness were decreased with increasing SiC contents (Fig. 4a and b). The deterioration of the mechanical properties should be caused by the decreased relative density. Under the hot pressing conditions of 1200 °C with 25 MPa, the 5 vol. %SiC/MoAlB composite has a relative density of 92.6%, close to 93 % for MoAlB material. Whereas the 15 vol. %SiC/MoAlB composite has a low relative density of 83.8%. Further increase of hot-pressing temperature to 1250 °C didn't contribute to the improvement in the density of composites.

The fracture surface demonstrates that the fracture mode is mainly transgranular (Fig. 5a). Cracks are deflected in the MoAlB grains due to its nanolaminated structure, but the transgranular crack path in the brittle and hard SiC grains is relatively flat. The nanolaminated structure of MoAlB can prolong the crack propagation paths, consuming more energy as cracks propagate in the grains, and thus endowing MoAlB with good damage tolerance and thermal shock resistance [15]. Figure 5b further illustrates the crack propagation path from the indentation corner. It can be found that the hard SiC particles play roles of "bridging", "pinning" and "deflecting" cracks in the crack propagation resistance.

The above results confirm that the incorporation of 5 vol. % SiC reinforcement in MoAlB is preferred and its strengthening effect is obvious. Therefore, the following studied was focused on the 5 vol. %SiC/MoAlB composite.

3.3 Oxidation behavior

Figure 6a depicts the oxide scale thickness as a function of time after oxidation at 1200°C and 1300°C for 10 h in air. The scale thicknesses of SiC/MoAlB are lower than those of MoAlB, i.e., 2.0 μm *vs* 2.7 μm after oxidation at 1200°C, and 3.9 μm *vs* 5 μm after oxidation at 1300°C, respectively. This result indicates that the scale growth rate on the SiC/MoAlB samples is slower than that on the MoAlB samples. The cross-sectional back-scattered SEM micrographs present the continuous oxide scales after oxidation at 1200°C (Fig. 6b) and 1300°C (Fig. 6c). The formed scales are thin and dense, and mainly composed of Al_2O_3.

The XRD result demonstrates that Al_2O_3 was the main oxide phase after oxidation at 1200°C (Fig. 7a). Diffraction peaks with strong intensities belonging to MoAlB were detected, further confirming the thinner scale. No SiC peaks were detected, suggesting that some SiC were oxidized and the residual SiC with content exceeded the detection limit of XRD. A broaden peak with low intensity locating at the diffraction angle of about 20° may be induced by the amorphous SiO_2 (Fig. 7a). The morphologies of oxides on the composite are illustrated in Fig. 7b-d. On the oxidized surface, SiO_2 particles are larger, while Al_2O_3

particles are smaller and irregular. The two phases are confirmed by XRD and EDS (Fig. 7d). The surfaces of SiO_2 particles are smooth, suggesting the viscous phase formed at above 1200°C. Small pores formed in the Al_2O_3 scale are irregular, whereas these formed in the SiO_2 particles are round. The appearance of round pores confirms that the evaporation of gas phases from the liquid SiO_2 phase upon oxidation at high temperatures. It should be noted that the pores became much round in the SiO_2 particles after oxidation at 1300°C (Fig. 7c). This feature suggests that the higher the temperature, the lower the viscosity of the formed SiO_2 glass phase and the easier it will flow. The formation of the viscous SiO_2 glass phase at high temperature is beneficial to seal the panels for the inward diffusion of O and the outward diffusion of elements from the matrix, contributing to the improvement of oxidation resistance especially at the early stage of oxidation.

4. Discussion

Fully dense MoAlB bulk samples are not easy to obtain under hot pressing conditions, possibly due to the existence of small pores caused by the evaporation of MoO_3 or B_2O_3 formed with the absorbed O at sintering temperatures. For example, a relative density of 94 % was achieved for the MoAlB samples by hot pressing of MoB and Al powders at 1200°C with 39 MPa for 5.8 h in vacuum [3]. In the present study, a relative density of about 93% for MoAlB prepared by hot pressing of a mixture of Mo, Al and B at 1200°C with 25 MPa for 1 h in Ar. No full density obtained in the SiC/MoAlB composites should be not only ascribed to the above reason, but also to the absence of sintering reactions between SiC and MoAlB phases. This has been confirmed by the SEM and TEM examinations (Figs. 2 and 3). The densification of composites without sintering reactions has always been a major challenge. For example, relative densities of 94.4% and 95% were obtained, respectively, in monolithic CrB_2 and 5 wt. % $MoSi_2/CrB_2$ composite after hot pressing at 1400 °C under 35 MPa for 2 h [16]. To further increase the density of SiC/MoAlB composites, hot isostatic pressing should be considered. It is reasonable to believe if the density of SiC/MoAlB composite was improved, the oxidation resistance would be further enhanced.

Upon high temperature oxidation, it is reasonable to assume the following oxidation reactions are:

$$2MoAlB\ (s) + 6O_2\ (g) = Al_2O_3\ (s) + B_2O_3\ (g) + 2MoO_3\ (g)\ (1)$$

$$SiC\ (s) + 2O_2\ (g) = SiO_2\ (s) + CO_2\ (g)\ (2)$$

For reaction (1), the sequence of phase formation at temperatures below 1400°C is $Al_2O_3 > B_2O_3 > MoO_3$ [17]. Before the formation of a dense and continuous Al_2O_3 scale, B_2O_3 and MoO_3 evaporate, and thus cause the weight loss upon oxidation at temperatures above 1200°C [18]. Once the dense and continuous Al_2O_3 scale formed, it acted as a barrier to prevent the inward diffusion of O and the outward diffusion of B and Mo, decreasing the evaporation rate of MoO_3 and B_2O_3. Therefore, the weight gain was predominant in the MoAlB material during oxidation at high temperatures.

For the oxidation of SiC/MoAlB composites, both reactions (1) and (2) occur. The reaction (2) induces a fluid glassy phase of SiO_2 at above 1200°C [19]. This fluid phase fills some pores and accelerates the formation of dense and continuous oxide scale, decreasing the oxidation rate and leading to the thinner oxide scale on the SiC/MoAlB as compared to the pure MoAlB material.

A cross-sectional back-scattered SEM micrograph presents the microstructure of scale. It should be noted that the formed SiO_2 was just over a SiC particle (Fig. 8a), confirmed by the EDS mapping (Fig. 8b). This feature suggests that the SiC particles on the surface is gradually oxidized to SiO_2. The small and round pore can be found in the SiO_2 particle, which should be resulted from the evaporation of gas phases of CO_2 according to Eq. (2) at 1300°C. In addition, it can be concluded that the larger SiC particles induce both the larger SiO_2 particles and pores formed at high oxidation temperatures on the basis of the microstructures shown in Figs. 7 and 8. It is reasonable to believe that fine SiC particles in the MoAlB will further improve the oxidation resistance of composites due to the fact that the fine reinforcement leads to the rapid formation of SiO_2 which seal the panels in the Al_2O_3 scale to retard the evaporation of B_2O_3 and MoO_3 in the initial oxidation stage.

Based on the above results, a proposed oxidation resistance mechanism for SiC/MoAlB was present in Fig. 9. Before a continuous Al_2O_3 and SiO_2 scale formation, the evaporation of MoO_3, B_2O_3, and CO_2 at above 1200°C induces the weight loss at early oxidation stage. However, the fluid glass of SiO_2 formed at above 1200°C can fill phase boundaries and small pores to seal the channels for the inward diffusion of oxygen. Hence, the oxidation resistance of SiC/MoAlB is better than that of MoAlB even at early oxidation stage. Once the continuous and dense scale forms, the inward diffusion rate of oxygen is retarded, and a low oxygen partial pressure under the scale generates. As a result, the oxidation of Mo and B followed by evaporation of MoO_3 and B_2O_3 is suppressed leading to weight gain. In addition, the fluid glass of SiO_2 can also heal microcracks and small pores in the scale, and further increase the bonding strength between the oxide scale and the matrix. This explains the reason why SiC/MoAlB has thinner dense oxide scales than MoAlB after oxidation at 1200°C and 1300°C.

5. Conclusions

5–15 vol.% SiC/MoAlB have been prepared by hot-pressing of SiC and MoAlB at 1200°C under 25 MPa for 1 h in Ar atmosphere. Such hot-pressing condition has resulted only 92.6 % theoretical density in 5 vol. %SiC/MoAlB composite, close to 95% for MoAlB. SiC and MoAlB are chemically stable without any reaction product at the sintering temperature of 1200°C. SiC as a reinforcing phase renders the 5 vol. %SiC/MoAlB composite stronger and harder. A flexural strength of 380 MPa and a Vickers hardness of 12.7 GPa were achieved in the 5 vol. %SiC/MoAlB composite, increased by 24% and 51%, respectively, as compared with those for MoAlB. In addition, the incorporation of SiC also improves the oxidation resistance of MoAlB due to the formation of a dense and continuous scale composed of Al_2O_3 and SiO_2, which prevents oxygen inward diffusion and the evaporation of oxides.

6. Declarations

Acknowledgements

This work was supported by National Natural Science Foundation of China under Grant no. 51772020, and Beijing Government Funds for the Constructive Project of Central Universities.

7. References

1. Ade M, Hillebrecht H. Ternary borides Cr_2AlB_2, Cr_3AlB_4 and Cr_4AlB_6: the first members of the series $(CrB_2)_nCrAl$ with *n* = 1, 2, 3 and a unifying concept for ternary borides as MAB-phases, *Inorg Chem* 2015, **54**: 6122-6135.
2. Kota S, Sokol M, Barsoum MW. A progress report on the MAB phases: atomically laminated, ternary transition metal borides, *Int Mater Rev* 2020, **65**: 226-255.
3. Mou JJ, Li SB, Yao BX, Ma PF, Yu WB, Zhou Y, Smokovych I, Scheffler M. Cyclic oxidation behavior of MoAlB in the temperature range 400-800 ºC, *J Alloy Compd* 2020, **831**: 154802
4. Kota S, Zapata-Solvas E, Ly A, Lu J, Elkassabany O, Huon A, Lee WE, Hultman L, May SJ, Barsoum MW. Synthesis and characterization of an alumina forming nanolaminated boride: MoAlB, *Sci Rep* 2016, **6**: 26475-26483.
5. Xu L, Shi O, Liu C, Zhu D, Grasso S, Hu C. Synthesis, microstructure and properties of MoAlB ceramics, *Ceram Int* 2018, **44**: 13396-13401.
6. Basu, S, Obando, N, Gowdy, A, Karaman, I, Radovic M. Long-term oxidation of Ti_2AlC in air and water vapor at 1000-1300 °C temperature range, *J Electrochem Soc* 2012, **159**: C90-96.
7. Li SB, Chen XD, Zhou Y, Song GM. Influence of grain size on high temperature oxidation behaviour of Cr_2AlC ceramics, *Ceram Int* 2013, **39**: 2715-2721.
8. Yao BX, Li SB, Ma PF, Zhang WW, Yu WB, Zhou Y. Oxidation behavior of $MoAl_{0.97}Si_{0.03}B$ solid solution at 1200-1400 °C, *Mater Today Commun* 2020, **22**: 100846.
9. Ma PF, Li SB, Hu J, Lu XG, Yu WB, Zhou Y. Processing and characterization of $MoAl_{1-x}Si_xB$ solid solutions, *J Alloys Compd* 2020, **814**: 152290.
10. Li SB, Xie JX, Zhang LT, Cheng LF. Mechanical properties and oxidation resistance of Ti_3SiC_2/SiC Composite by *In Situ* Displacement reaction of Si and TiC, *Mater Lett* 2003; **57**: 3048-3056.
11. Li SB, Song GM, Zhou Y. A dense and fine-grained SiC/$Ti_3Si(Al)C_2$ composite and its high-temperature oxidation behavior, *J Euro Ceram Soc* 2012, **32**(12): 3435-3444.
12. Barsoum MW, Ho-Duc LH, Radovic M, El-Raghy T. Long time oxidation study of Ti_3SiC_2, Ti_3SiC_2/SiC and Ti_3SiC_2/TiC composites in air, *J Electrochem Soc* 2003, **150**: B166-175.
13. Wan DT, Zhou YC, Hu CF, Bao YW. Improved strength-impairing contact damages resistance of $Ti_3Si(Al)C_2$/SiC composites, *J Eur Ceram Soc* 2007, **27**: 2069-2076.

14. Zhang J, Wang L, Jiang W, Chen L. High temperature oxidation behavior and mechanism of Ti_3SiC_2-SiC nanocomposites in air, *Comp Sci Tech* 2008, 68: 1531-1538.
15. Zhou X, Jing L, Kwon YD, Kim JY, Huang Z, Yoon DH, Lee J, Huang Q. Fabrication of SiC_w/Ti_3SiC_2 composites with improved thermal conductivity and mechanical properties using spark plasma sintering, *J Adv Ceram* 2020, **9(4)**: 462-470.
16. Lu XG, Li SB, Zhang WW, Yu WB, Zhou Y. Thermal shock behavior of a nanolaminated ternary boride: MoAlB, *Ceram Int* 2019, **45**: 9386-9389.
17. Reddy V, Sonber JK, Sairam K, Murthy TSRCh, Kumar S, Nageswara Rao GVS, Srinivasa Rao T, Chakravartty JK. Densification and mechanical properties of CrB_2+$MoSi_2$ based novel composites, *Ceram Int* 2015, **41**: 7611-7617.
18. Lu XG, Li SB, Zhang WW, Yao BX, Yu WB, Zhou Y. Crack healing behavior of a MAB phase: MoAlB, *J Euro Ceram Soc* 2019, **39**: 4023-4028.
19. Mou J, Li S, Yao B, Ma P, Yu W, Zhou Y, Smokovych I, Scheffler M. Cyclic oxidation behavior of MoAlB in the temperature range 400-800 ºC, *J Alloy Compd* 2020, **831**: 154802.
20. Li S, Song G, Zhou Y. A dense and fine-grained SiC/$Ti_3Si(Al)C_2$ composite and its high-temperature oxidation behavior, *J Euro Ceram Soc* 2012, **32**: 3435-3444.

Figures

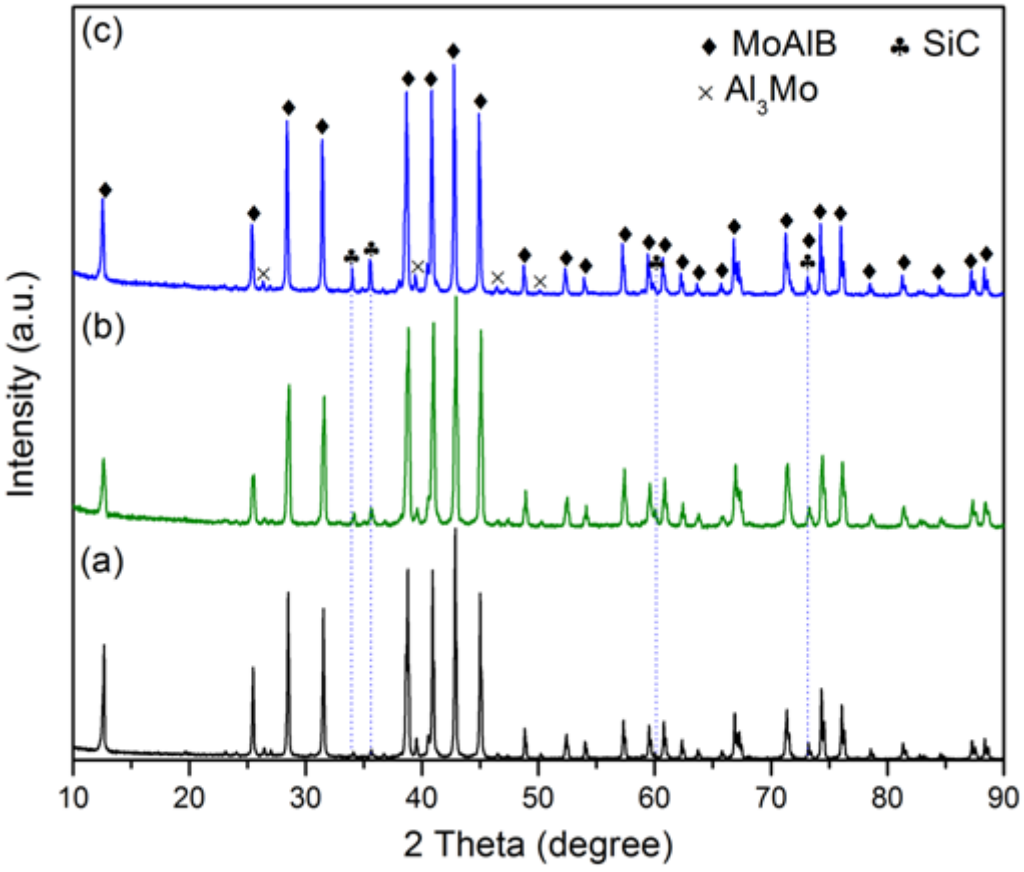

Figure 1

XRD patterns of (a) 5 vol.%, (b) 10 vol.%, and (c) 15 vol.% SiC/MoAlB composites

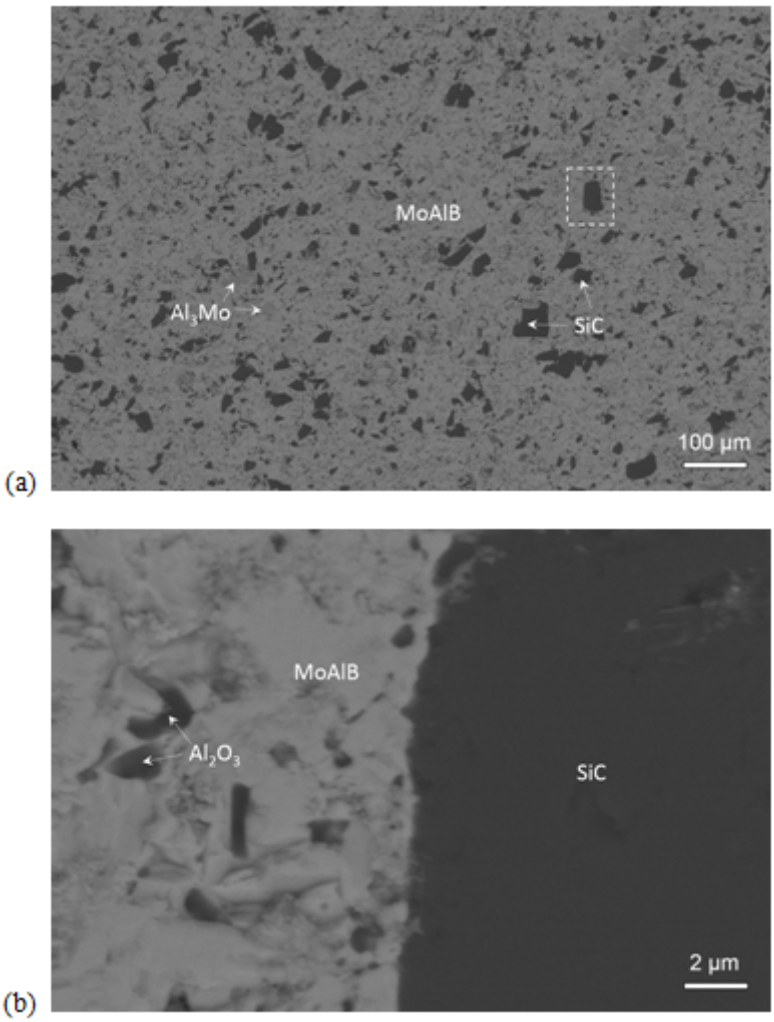

Figure 2

Back-scattered SEM micrographs of the polished surface of 10 vol.% SiC/MoAlB. (a) A low magnification image, (b) A high magnification image taken from (a).

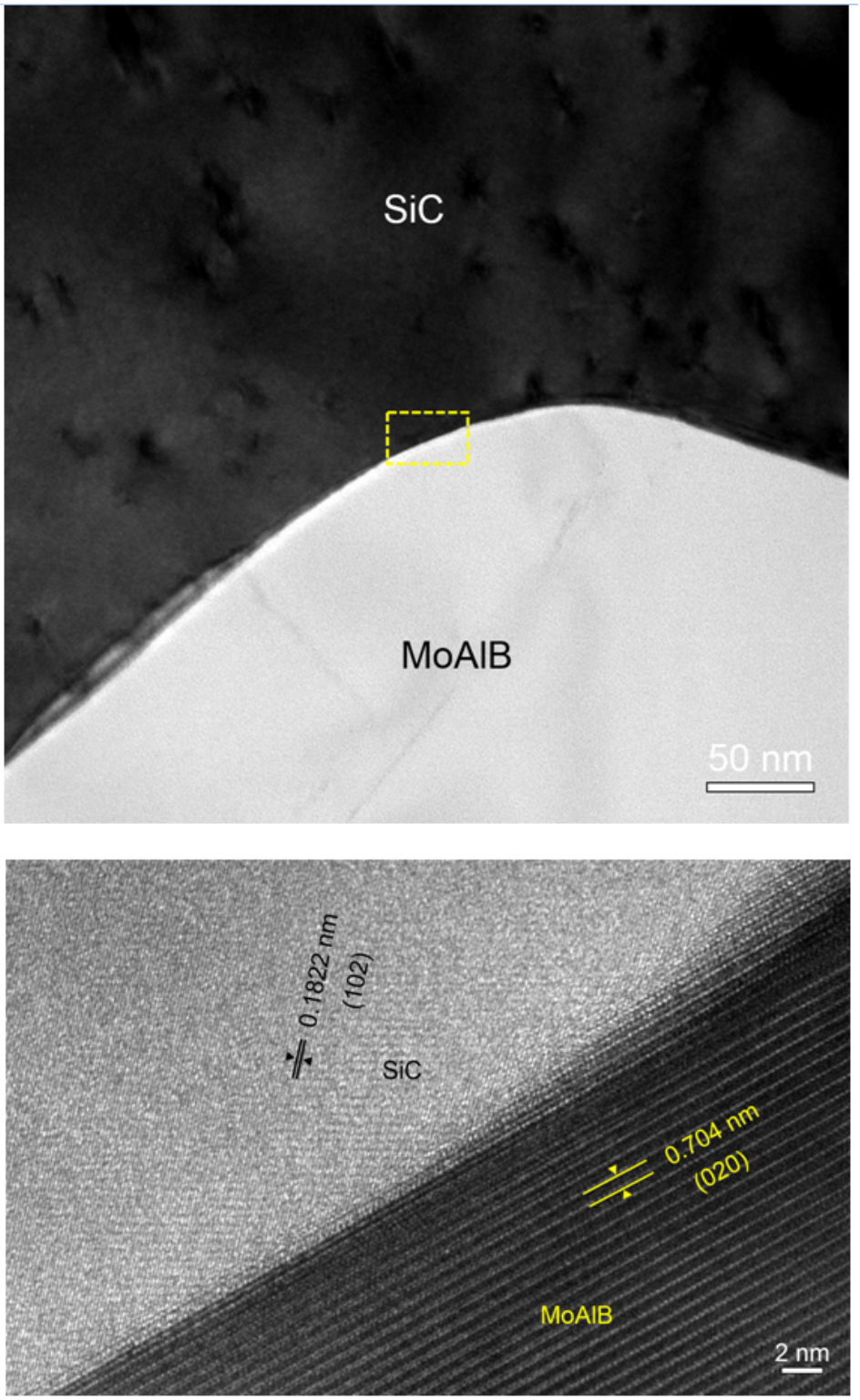

Figure 3

(a) TEM image of SiC/MoAlB, and (b) HRTEM image of the zone marked with a dashed rectangle in (a).

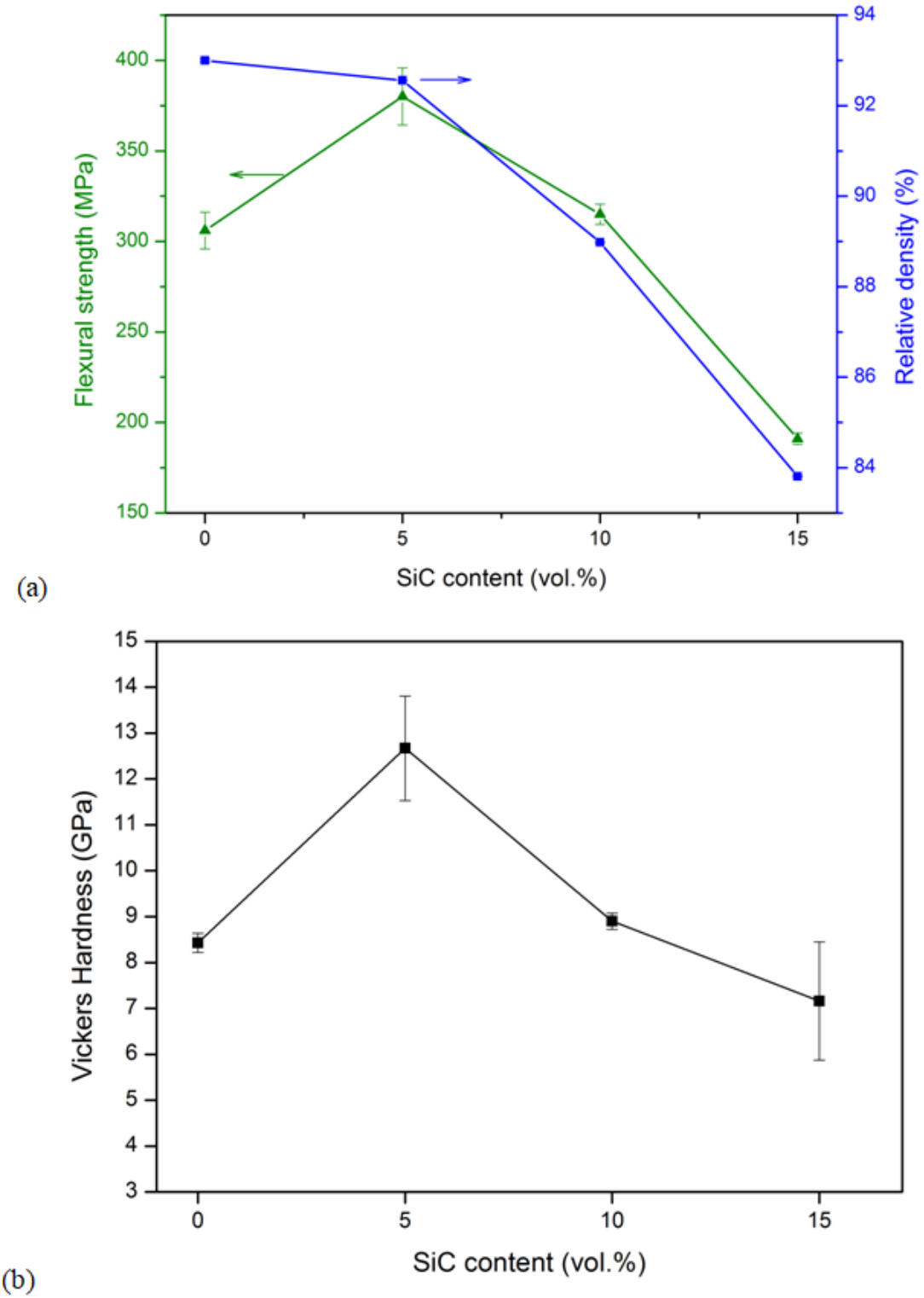

Figure 4

Mechanical properties of SiC/MoAlB composites, together with those of MoAlB and MoAl0.97Si0.03B for comparison. (a) Flexural strength, and (b) Vickers hardness.

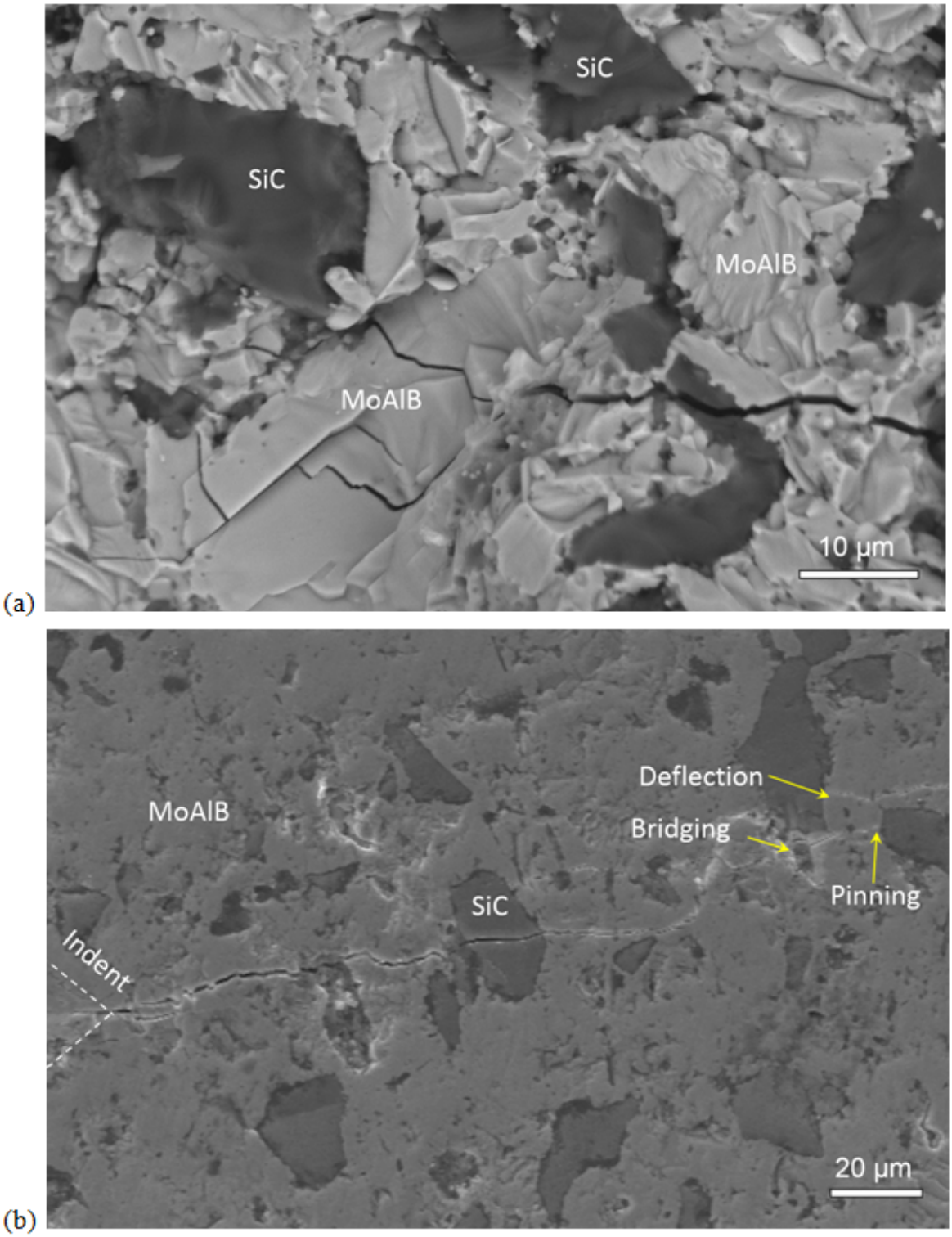

Figure 5

SEM micrographs of crack propagation paths in the 5 vol.% SiC/MoAlB composite. (a) A back-scattered electron image of the fractured surface, and (b) A second electron image of a crack emanating from the indentation corner.

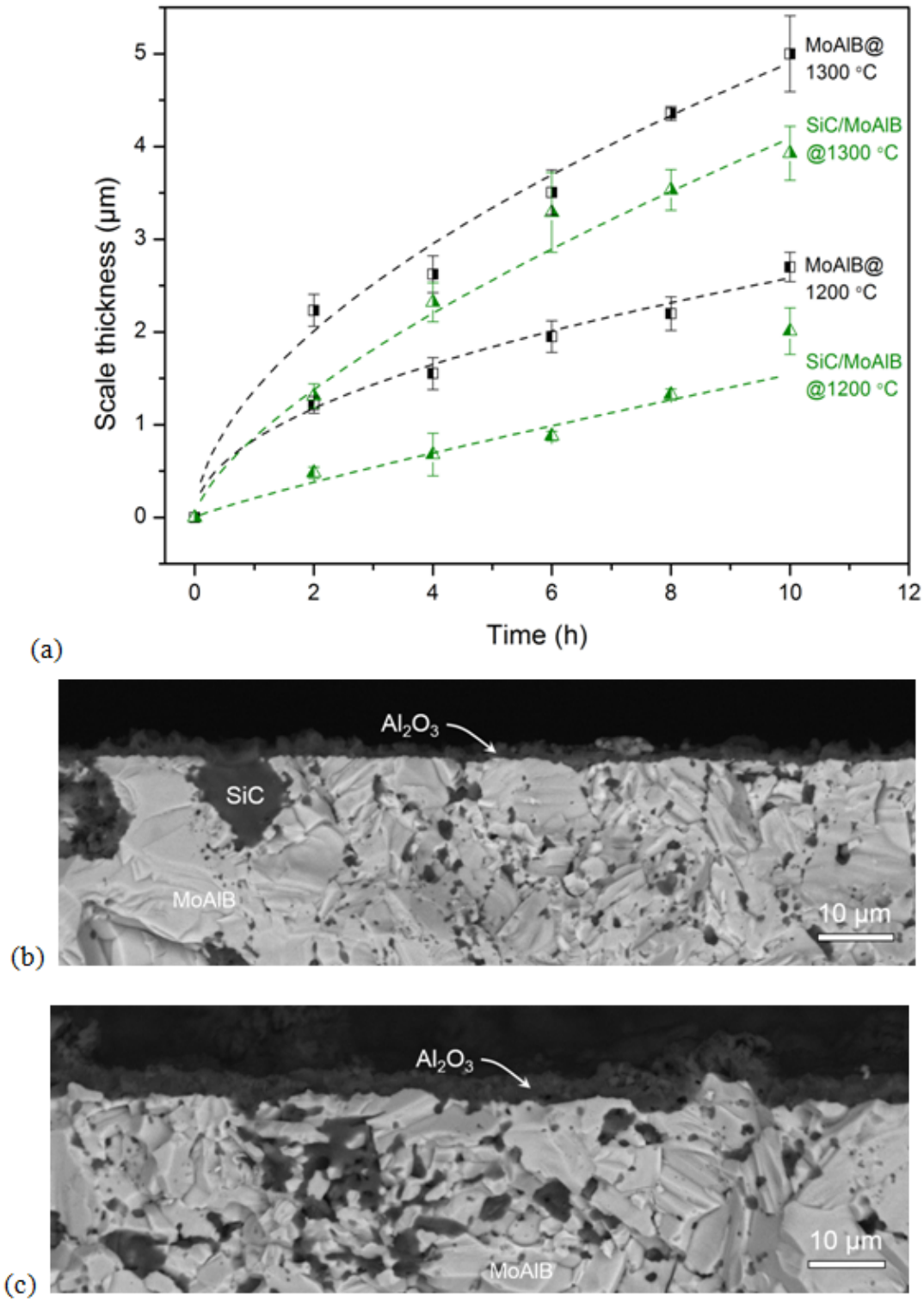

Figure 6

Scale thickness as a function of oxidation time for 5 vol.% SiC/MoAlB composite (a), and Cross-sectional back-scattered SEM micrographs of the composite after oxidation at (b) 1200 ºC and (c) 1300 ºC for 10 h in air.

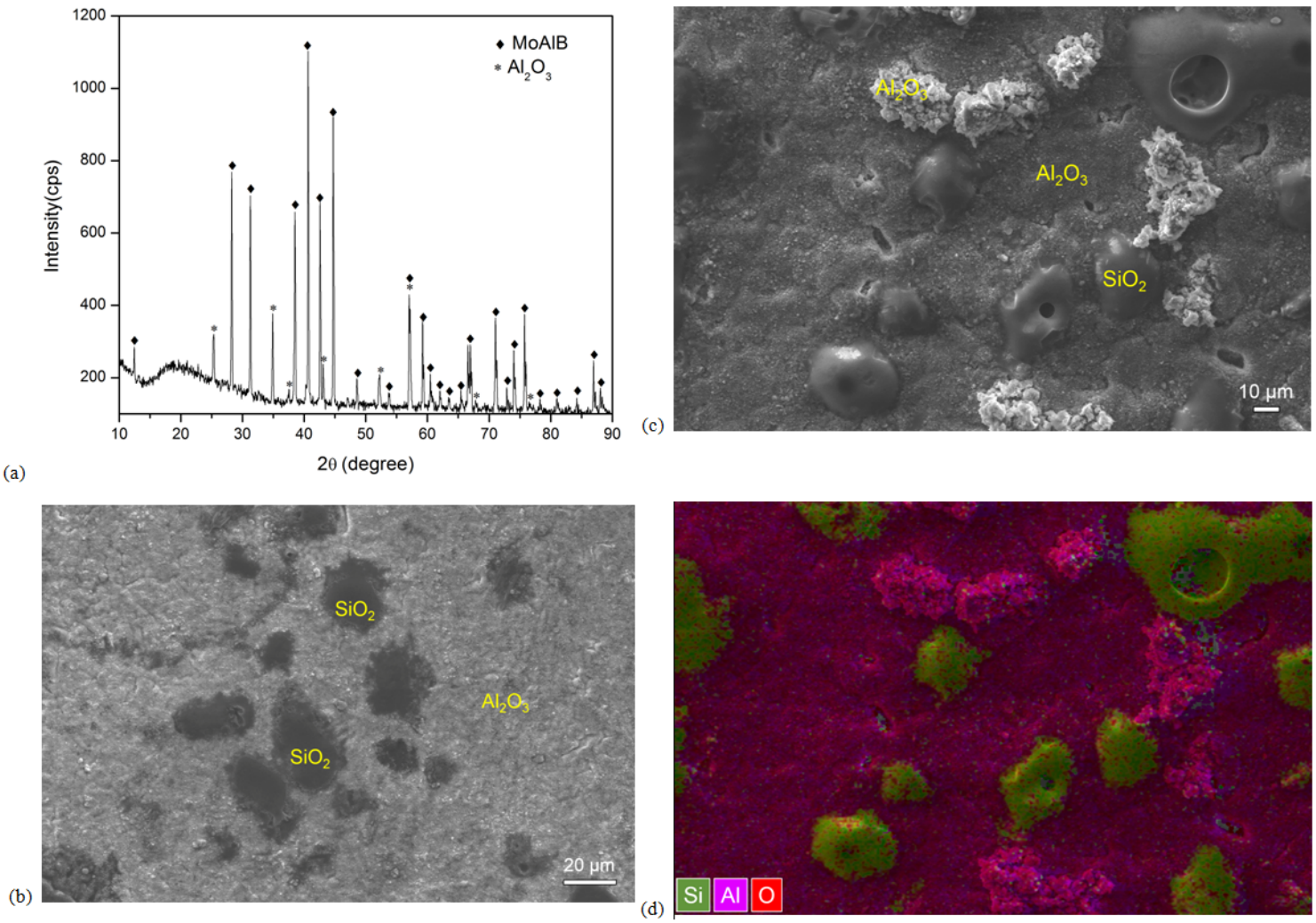

Figure 7

(a) XRD pattern of 5 vol.% SiC/MoAlB composite after oxidation at 1200 C for 10 h, SEM micrographs of oxides on the composite after oxidation at (b) 1200 °C and (c-d) 1300 °C for 10 h in air. (d) is the EDS mapping for (c).

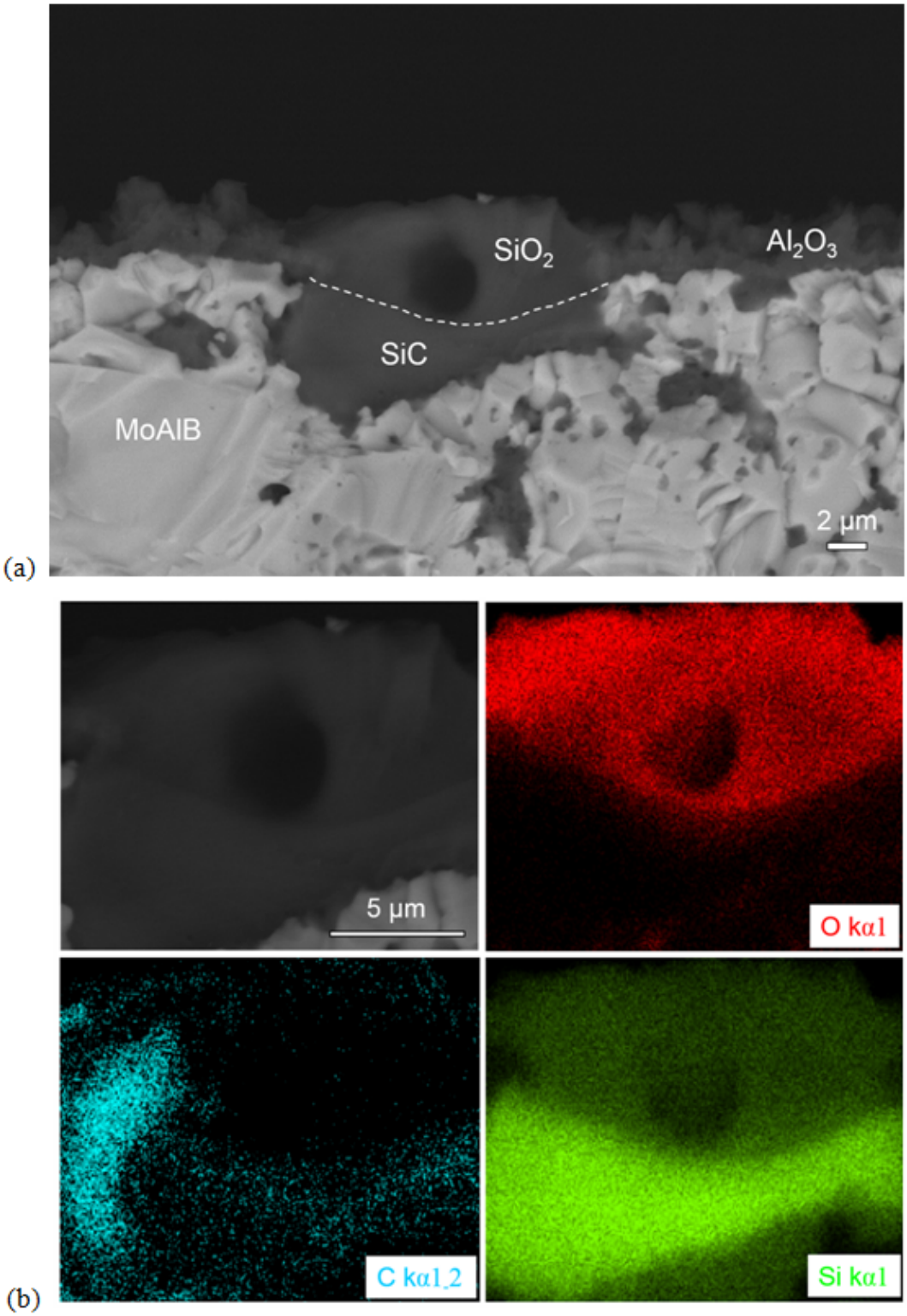

Figure 8

Cross-sectional back-scattered SEM micrograph (a), and corresponding EDS mapping (b) of 5 vol.% SiC/MoAlB composite after oxidation at 1300 ºC for 10 h in air.

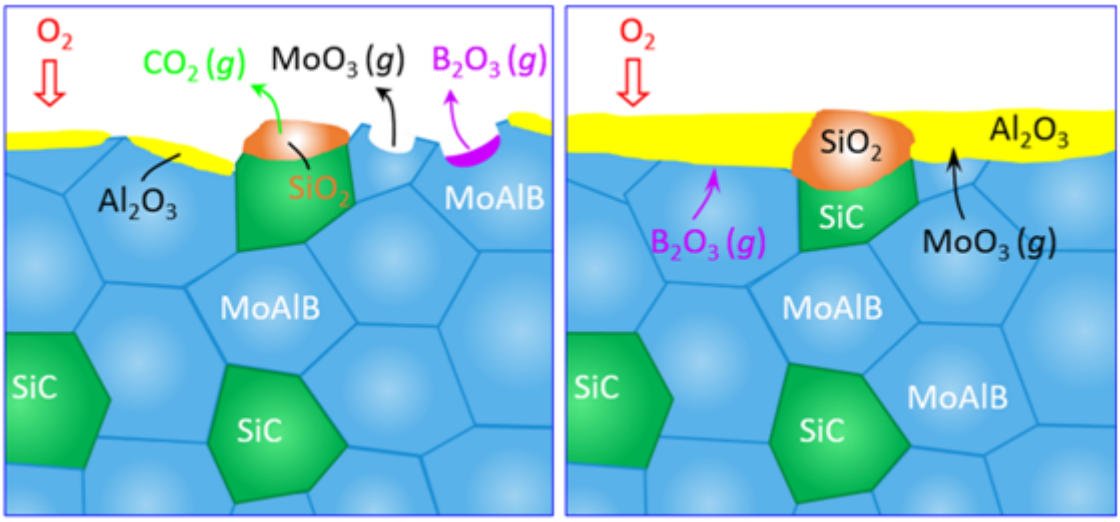

Figure 9

Schematic of the oxidation process mechanism of SiC/MoAlB when exposed to air.